AD-A052 096   NAVAL RESEARCH LAB WASHINGTON D C   F/G 17/1
MASSA TR-11C TRANSDUCERS - HYDROSTATIC PRESSURE TESTS.(U)
FEB 61 G PIDA

UNCLASSIFIED   NRL-MR-1148   NL

1 OF 1
ADA
052096

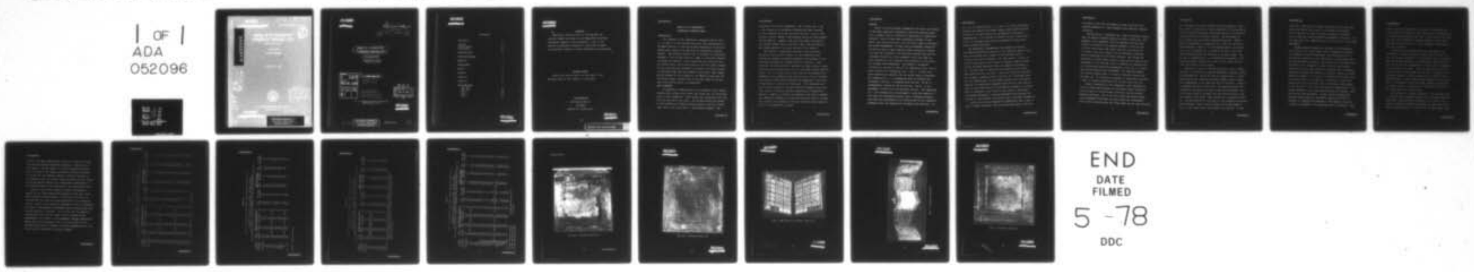

END
DATE
FILMED
5-78
DDC

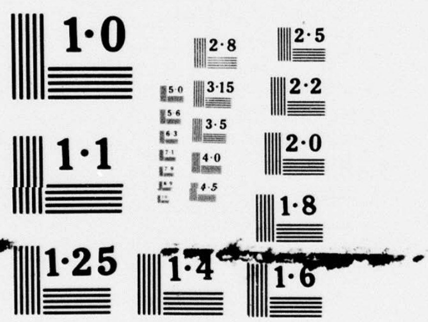
1·0
2·8
2·5
5·0
3·15
2·2
5·6
3·5
6·3
2·0
1·1
7·1
4·0
4·5
1·8
1·25
1·4
1·6

UNCLASSIFIED

[redacted]

NRL Memorandum Report

MASSA TR-11C TRANSDUCERS - HYDROSTATIC PRESSURE TESTS

[Unclassified Title]

George Pida

SOUND DIVISION

February 23, 1961

U. S. NAVAL RESEARCH LABORATORY
Washington, D.C.

4050792-61

UNCLASSIFIED

[redacted]

UNCLASSIFIED

[redacted]

(9) NRL Memorandum Report, 1148

(14) NRL-MR-1148

(6) MASSA TR-11C TRANSDUCERS - HYDROSTATIC PRESSURE TESTS.

(Unclassified Title)

(10) George/Pida

Transducer Branch
Sound Division

ACCESSION for		
NTIS	White Section	X
DDC	Buff Section	☐
UNANNOUNCED		☐
JUSTIFICATION Per Ltr. on file		
BY		
DISTRIBUTION/AVAILABILITY CODES		
Dist.	AVAIL. and/or SPECIAL	
A		

(11) 23 February 23, 1961

(12) 22p.

(16) F00103

(17) SF00103 04

U. S. Naval Research Laboratory
Washington, D. C.

UNCLASSIFIED

[redacted]

251950

DISTRIBUTION STATEMENT A
Approved for public release;
Distribution Unlimited

4050792-61

TC

CONTENTS

UNCLASSIFIED

[redacted]

ABSTRACT

Hydrostatic pressure tests in the NRL 8000 psi pressure chamber were made on four Massa TR-11C variable reluctance, magnetic field transducers. Some of the effects of hydrostatic pressure on structural strength and functional behavior of these transducers are discussed.

PROBLEM STATUS

This is an interim report on this phase of the problem; work on other phases is continuing.

AUTHORIZATION

NRL Problem S02-06

Task 8047

BuShips No. S-F001-03-04

UNCLASSIFIED

[redacted]

MASSA TR-11C TRANSDUCERS - HYDROSTATIC PRESSURE TESTS

INTRODUCTION

Four magnetic field transducers, designated TR-11C, Nos. 1, 2, 3 and 4, of the variable reluctance type manufactured by The Massa Division of Cohu Electronics Corporation for Project Artemis were tested in the NRL 8000 psi hydrostatic pressure chamber. The principal purpose was to determine the structural strength of the box walls and any change in functional behavior that might be observed. These transducers are different from the TR-11B series with hollow plates in that the plates forming the box enclosure were rabbeted to provide a structural support of each plate edge onto each adjacent plate edge. This change avoids reliance on the strength of the adhesive bonds only for structural support between some of the plate edges as was the case in the TR-11B series of transducers.

TEST PROCEDURE

In preparing the Massa units for the pressure test a rubber molding with a brass sleeve insert was molded onto the electrical cable of each transducer. This molding was placed about six feet from the free end of the cable. The molding served the purpose of the stuffing in a regular stuffing gland to provide a water-tight seal at the cable entry of the pressure chamber. The transducers were tested separately. Two of them, Nos. 1 and 3, were subjected to pressures exceeding the plate strength of the transducer walls and the other two, Nos. 2 and 4, were pressure cycled. Number 2 was pressure cycled 45 times between 250 and 2000 psi. Number 4 was cycled 50 times over each of four ranges between 200 psi and 1700, 1800, 1900 and 2000 psi. The average period of one cycle was about four minutes.

The effects of hydrostatic pressure on the structural stability and functional behavior of the transducers were detected by changes in measured impedance and frequency of the principal and parasitic resonant modes of vibration. Some structural failures were also indicated by sharp, audible sounds resulting from an implosion of the box that were readily detected by ear. At low driving levels (less than one milliampere) the impedance of the transducer was measured with a vector impedance locus plotter (VILP) which indicates the magnitude of the X and R components as a function of frequency. This instrument was used to detect parasitic resonant modes and changes in the principal modes of vibration caused by application of hydrostatic pressure. Ammeter, voltmeter and wattmeter were used to measure the transducer impedance at higher driving levels and to continuously monitor the frequency at maximum impedance during application of the hydrostatic pressure.

RESULTS

Unlike the previous Massa transducers that have been checked at NRL under hydrostatic pressures, these four developed parasitic resonant modes of vibration on application of hydrostatic pressure. Some of these modes persisted, although, in most cases, with reduced activity, over the entire range of pressures and others disappeared. In each case at pressures between 100 and 300 psi some of these parasitic modes occurred at frequencies near the frequency of the principal resonant mode and the consequent distortion of the impedance circle plot made the usual evaluation of Q, frequency, and resistance of the principal resonant mode meaningless. The parasitic resonances occurred at a pressure of 300 psi for transducers, Nos. 1 and 2, and at 100 psi for transducers, Nos. 3 and 4. In each case these modes did not persist over the entire range of pressures. For transducer No. 1, it disappeared when the pressure was decreased to 250 psi or increased above 320 psi. For No. 2, disappearance occurred at 220 and 400 psi. For No. 4, disappearance occurred at 60 psi and above 300 psi. For transducer No. 3, the pressure was not decreased to learn the behavior of this mode for decreasing pressure, and on increasing pressure this mode only diminished in its activity and did not completely disappear until the pressure was increased above 1000 psi. In the case of transducers Nos. 1, 2, and 4, on which the applied pressure was reduced from higher values, these parasitic modes recurred at the same pressure as originally in the case of transducer No. 1 but recurred at 200 psi for No. 2 and 70 psi for No. 4, somewhat lower than the pressures at which these modes occurred originally.

The appearance, disappearance and changes in activity with applied hydrostatic pressure of the parasitic modes occurring off-resonance with respect to the principal mode of vibration are given in Tables I, II, III, and IV. It will be noted in each table in the column of frequency under the heading "At Principal Resonance" that the change in frequency of the principal mode of vibration with pressure alone, in the range above 500 psi, was about 1 cycle per second for each 200 psi increase in pressure when excited at the low driving level that the VILP allows. At the higher driving level (100 milliamperes), at hydrostatic pressures above 500 psi, this rate is about 2 cycles per second for each 200 psi increase in pressure. This is indicated in each table in the column of data under the heading "Frequency of Maximum Impedance" and includes the effects of both pressure and driving level on resonant frequency.

Cycling the pressure applied to transducers, Nos. 2 and 4, had no effects different from the initial application over the same range except that the parasitic modes associated with pressure appeared at a lower pressure level than was observed initially.

The enclosure of transducer No. 1 had a structural failure when the applied pressure reached the value of 2650 psi. The diameter of the impedance circle as measured with the VILP started to decrease at the applied pressure of 2100 psi and in effect anticipated that plate deflection was sufficient to produce very light contact with the internal moving mass but not sufficient for structural failure. The failure was indicated by several sharp, audible sounds and by complete disappearance of the principal mode of vibration as observed with the continuously monitoring instruments at the time of failure and with the VILP shortly afterwards. The VILP also showed that several higher modes of vibration developed between 1000 and 2000 cps. On reducing the pressure to atmospheric pressure, a mode of vibration appeared at 413 cps and one at 491 cps.

Visual observation of this transducer, after removing the rubber covering and removing the four hollow plates constituting four walls of the enclosure, showed all plates were permanently deflected. Two of the four plates had barely perceptible permanent deflection, the third plate had considerably more visible deflection and the fourth plate was not only deflected but fractured as is quite evident in the photographs of Fig. 1. The latter two plates also showed separation of the two waffle halves composing the plate, indicating failure of the adhesive bond that holds the sections together. The photograph in Fig. 2 shows the two sections composing the plate. Figure 3 shows the appearance of transducer No. 3 with the four hollow plates removed. Figure 4 is a photograph taken of one radiating end of transducer No. 3 giving an outline of the plate edges showing clearly the rabbeting of the plate edges. One air gap of transducer No. 1, as measured after removal of the enclosure plates, varied from 0.024 to 0.027 inches and the other from 0.027 to 0.031 inches.

Structural failure of the enclosure wall plates of transducer No. 3 occurred at an applied hydrostatic pressure between 2100 and 2200 psi. As in the case of transducer No. 1, structural failure was indicated by several sharp, audible sounds and disappearance of the principal mode of vibration. Instead of stopping the test at this point, the applied pressure was increased to determine the value at which the transducer electrical cable would be extruded from the stuffing gland in the test chamber cable entry. This occurred at a pressure of 8800 psi. As was expected all four walls of the transducer enclosure were fractured. This is quite evident in the photograph of Fig. 3. The plates were forced against the springs. In this test (up to 8800 psi) all cement bond joints of all four side plates and cement bond joints of all springs were broken. The end plates, from which acoustic radiation is produced, did not have any visibly perceptible permanent deflection. The air gaps were fairly uniform varying from 0.023 to 0.025 inches.

CONCLUSION

Although applied pressure at fracture of the transducer wall plates is an obvious upper limit of hydrostatic pressure for operation of these transducers, the limiting factor for satisfactory operation is the deflection of these plates with applied hydrostatic pressure. The deflection of the plate wall was equal to the clearance of about 1/8 of an inch between plates and the free mass inside the enclosure when the applied hydrostatic pressure was 2000 psi or higher, however, the plate deflection appears to be elastic (or reversible), judging from the cycling tests, up to 2000 psi. Firm proof of the latter supposition could be obtained only by attaching strain gauges to the box prior to the tests and before the application of the rubber covering of the element and measuring the strains. This test has not been attempted. Contact between internal and external parts produced a detectable change in the rate of decrease of frequency and diameter of the impedance circle at or near the resonance of the principal mode of vibration. This behavior was more pronounced in the case of transducer, No. 1, between applied pressures of 2000 and 2650 psi. Observation of the plates showed evidence that two of these plates, including one that did not fracture, deflected against the free mass structure with enough force to leave permanent depressions in the plate surfaces.

A satisfactory explanation has not been made for the development of parasitic modes of appreciable activity at or near the resonant frequency of the principal mode of vibration when the applied pressure on the transducers was between 100 and 300 psi, and the disappearance of these modes at pressures below and above this range. There was associated with this pressure range a marked change in the rate of decrease in the resonant frequency of the principal mode of vibration with applied pressure. This behavior might suggest that an elastic shift or realignment of the structural assembly, probably at the bonded joints, on application of hydrostatic pressures in this range may be the common cause.

The decrease in resonant frequency of the principal mode of vibration with increased driving level and with increasing hydrostatic pressure may be accounted for in terms of the change in negative stiffness introduced by change in the air gap flux density which is a function of air gap length. The effective air gap length depends upon the electrical driving level and the applied hydrostatic pressure. Computations of the change of air gap length at the 100 milliampere driving level in terms of the change in negative stiffness necessary to account for the observed change in resonant frequency of the principal mode of vibration agree favorably with the change in air gap length obtained from displacement measurements of the radiating mass of the transducer at the same driving level.

Finally, since this transducer element is designed to operate in an ambient hydrostatic pressure of 600 psig, these tests indicate a safety factor of more than three and it is believed that the units will have satisfactory life characteristics. Further tests should be performed in order to determine the cause of the parasitic resonances which are associated with ambient hydrostatic pressure. It is noted that the parasitic resonance at about 500 cps, which is also observed in air measurements, is a result of the mechanical design, employed by Massa, which omits springs on two of the four sides of the structure and allows a resonance or motion perpendicular to the motion used for radiation of acoustic energy.

TABLE I

Some of the Hydrostatic Test Data - Massa Transducer TR-11C, No. 1

Polarizing current = 9.5 amperes. Driving current at frequency of maximum impedance (Z_m) was 100 milliamperes. This frequency was well within the bandwidth of the principal mode of vibration.

Gauge Pressure in psi	Freq. of Z_m in cps	At Principal Resonance Freq. cps	Circle Dia. in ohms	Q	Parasitic Modes Freq. cps	Loop Dia. in ohms	Freq. cps	Loop Dia. in ohms	Freq. cps	Loop Dia. in ohms
(in air)	456	468	370	52	498	50	--	--	--	--
(in water)	432	449	500	64	491	20	--	--	--	--
40	430	444	500	74	496	10	--	--	--	--
100	430	444	470	56	496	10	471	10	--	--
180	428	444	480	56	495	10	470	10	--	--
200	429	444	500	56	490	10	448	20	--	--
250	--	446	440	50	502	20	450	60	424	40
300	425	Distorted Impedance Circle			498	20	451	80	433	100
320	425	435	300	54	494	10	450	100	--	--
400	425	436	370	73	503	10	455	80	451	80
500	423	436	390	73	500	10	457	70	450	70
600	422	435	420	54	496	10	457	60	450	60
800	420	435	470	62	495	10	458	50	450	50
1000	419	435	490	72	495	10	459	40	450	40
1200	417	433	530	72	490	10	459	30	451	30
1500	414	433	540	62	490	10	459	30	450	30
60	430	442	460	55	493	20	--	--	--	--
300	425	Distorted Impedance Circle			488	10	454	100	450	80
1600	413	432	520	62	484	20	458	20	450	10
1800	412	431	550	62	480	20	459	20	450	10
2000	408	428	520	54	--	--	467	60	450	5
2100	406	427	420	43	--	--	466	60	--	--
2200	404	425	390	43	--	--	463	70	--	--
2300	402	424	340	42	--	--	463	80	--	--
2400	401	423	220	30	--	--	461	70	440	20
2500	398	421	160	13	--	--	460	50	430	60
2600	394	438	210	27	--	--	460	40	418	40
2650	Plate fractured and principal mode disappeared.									

TABLE II

Some of the Hydrostatic Test Data - Massa Transducer TR-11C, No. 2

Polarizing current = 9.5 amperes. Driving current at frequency of maximum impedance (Z_m) was 100 milliamperes. This frequency was well within the bandwidth of the principal mode of vibration.

Gauge Pressure in psi	Freq. of Z_m in cps	At Principal Resonance					Parasitic Modes			
		Freq. cps	Circle Dia. in ohms	Q	Freq. cps	Loop Dia. in ohms	Freq. cps	Loop Dia. in ohms	Freq. cps	Loop Dia. in ohms
(in air)	453	467	430	47	501	60	--	--	--	--
(in water)	429	440	460	44	500	20	461	20	450	20
40	427	441	530	63	496	10	469	5	450	5
100	428	438	460	63	497	20	457	50	450	40
200	428	443	560	63	499	10	450	10	412	20
220	430	443	540	63	495	20	450	20	411	20
300	423	Distorted Impedance Circle			--	--	451	50	444	150
400	422	435	430	54	497	30	456	100	450	100
500	422	434	460	62	497	10	455	70	450	70
1000	41[illegible]	433	540	54	494	10	458	60	450	40
1700	408	429	560	54	484	20	458	50	450	20
2000	403	427	520	53	551	10	470	40	450	30
2000*	401	424	480	47	--	--	464	60	--	--
300	417	431	460	54	488	10	452	100	450	100
200	417	Distorted Impedance Circle			494	20	450	30	437	150
0	424	439	570	55	491	20	--	--	--	--
(in air)	448	463	450	46	496	50	--	--	--	--

*After 45 Pressure Cycles

TABLE III

Some of the Hydrostatic Test Data - Massa Transducer TR-11C, No. 3

Polarizing current = 9.5 amperes. Driving current at frequency of maximum impedance (Z_m) was 100 milliamperes. This frequency was well within the bandwidth of the principal mode of vibration.

Gauge Pressure in psi	Freq. of Z_m in cps	At Principal Resonance					Parasitic Modes			
		Freq. cps	Circle Dia. in ohms	Q	Freq. cps	Loop Dia. in ohms	Freq. cps	Loop Dia. in ohms	Freq. cps	Loop Dia. in ohms
(in air)	453	466	540	42	505	40	--	--	--	--
(in water)	425	438	540	50	502	10	465	5	--	--
40	425	440	675	50	493	10	--	--	--	--
100	421	Distorted Impedance Circle			500	10	454	80	441	80
200	418	Distorted Impedance Circle			494	10	451	50	443	200
300	419	432	460	54	503	10	450	100	--	--
400	418	433	500	54	502	10	455	100	450	100
500	417	433	520	54	503	10	455	70	451	70
700	415	432	560	62	500	10	455	60	450	60
1000	413	431	600	54	498	10	457	40	452	40
1500	406	429	600	48	490	10	457	30	450	20
1000	416	433	600	48	487	10	458	40	451	30
1500	411	430	600	54	486	10	459	20	451	20
2000	404	426	520	53	486	10	459	20	450	20
2100-2200	Sharp audible sound occurred indicating breakage of plate and principal mode of vibration disappeared. Increased pressure to 8800 psi when transducer electrical cable was extruded from stuffing gland in test chamber cable entry.									

TABLE IV

Some of the Hydrostatic Test Data - Massa Transducer TR-11C, No. 4

Polarizing current = 9.5 amperes. Driving current at frequency of maximum impedance (Z_m) was 100 milliamperes. This frequency was well within the bandwidth of the principal mode of vibration.

Gauge Pressure in psi	Freq. of Z_m in cps	At Principal Resonance Freq. cps	At Principal Resonance Circle Dia. in ohms	At Principal Resonance Q	Freq. cps	Loop Dia. in ohms	Parasitic Modes Freq. cps	Parasitic Modes Loop Dia. in ohms	Freq. cps	Loop Dia. in ohms
(in air)	446	464	430	46	498	60	--	--	--	--
(in water)	424	439	400	49	493	10	--	--	--	--
40	422	439	440	44	494	10	475	10	--	--
100	423	Distorted Impedance Circle			496	10	449	80	413	30
200	423	442	500	50	495	20	449	40	412	40
60	422	439	480	55	491	10	468	20	--	--
300	422	434	440	62	494	10	456	100	413	20
1000	411	431	530	61	495	10	460	40	411	30
1700	404	428	530	61	486	20	460	40	409	20
1700(1)	402	427	510	54	485	10	459	40	409	10
200(1)	413	431	480	61	491	10	453	40	411	20
1800(1)	403	426	490	53	--	--	462	30	409	20
1800(2)	400	426	450	53	--	--	467	30	409	20
200(2)	413	431	460	54	492	10	453	70	411	30
1900(2)	399	425	470	47	--	--	469	50	408	20
1900(3)	400	424	450	53	--	--	468	50	408	20
200(3)	414	430	500	61	496	10	453	60	411	20
90(3)	417	442	460	44	484	40	--	--	413	20
70(3)	Distorted Impedance Circle - largest parasitic loop at 441 cps									
200(3)	416	433	440	54	489	20	454	50	412	20
2000(3)	400	425	400	47	--	--	464	80	408	20
2000(4)	399	424	400	47	--	--	465	60	409	20
200(4)	412	430	480	61	488	10	454	50	411	20
200(5)	417	433	420	48	488	10	455	60	412	40
100(5)	417	434	340	43	492	20	450	30	413	20
0(5)	418	438	320	31	490	10	--	--	413	20
(in air)(5)	443	462	400	46	494	40	--	--	416	10

(1) After 50 Pressure Cycles
(2) After 100 Pressure Cycles
(3) After 150 Pressure Cycles
(4) After 200 Pressure Cycles
(5) Next day

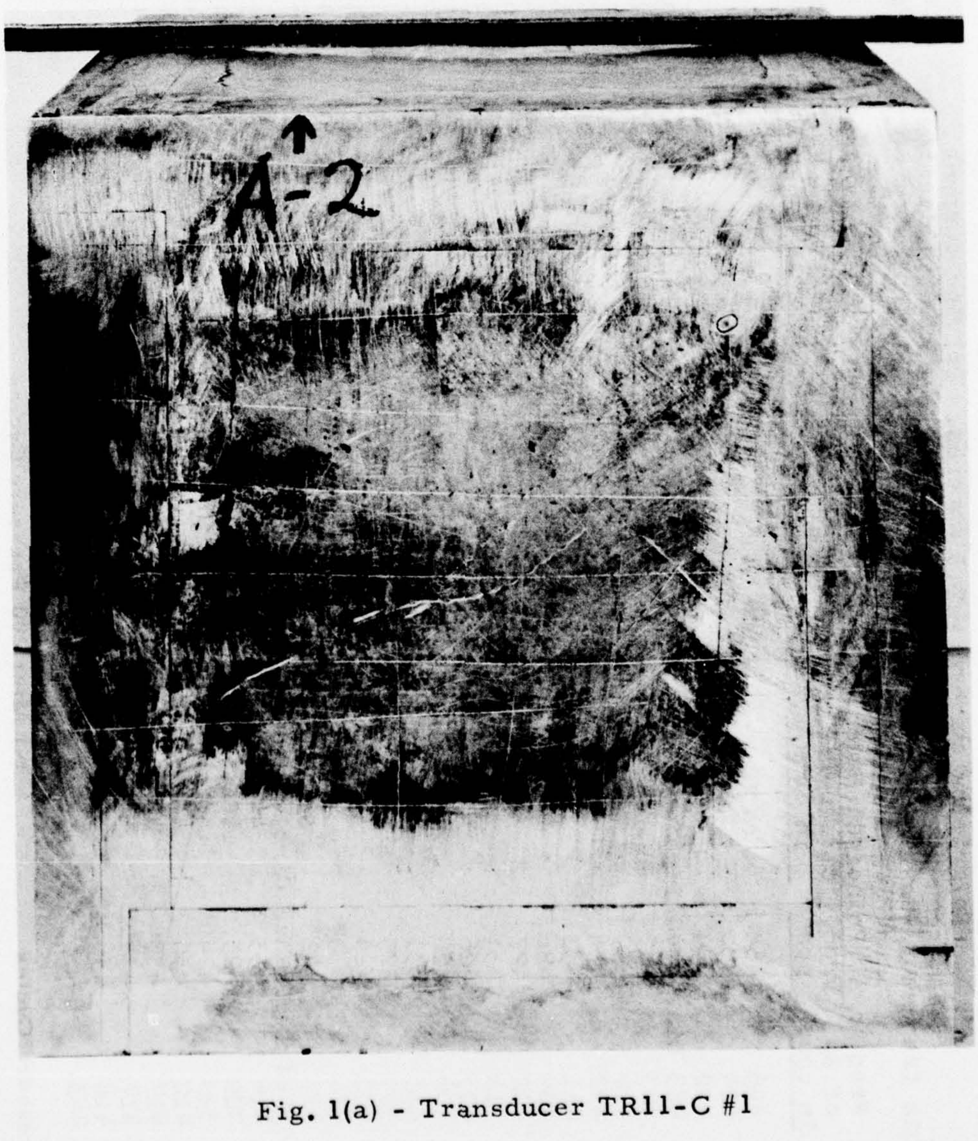

Fig. 1(a) - Transducer TR11-C #1

UNCLASSIFIED

[redacted]

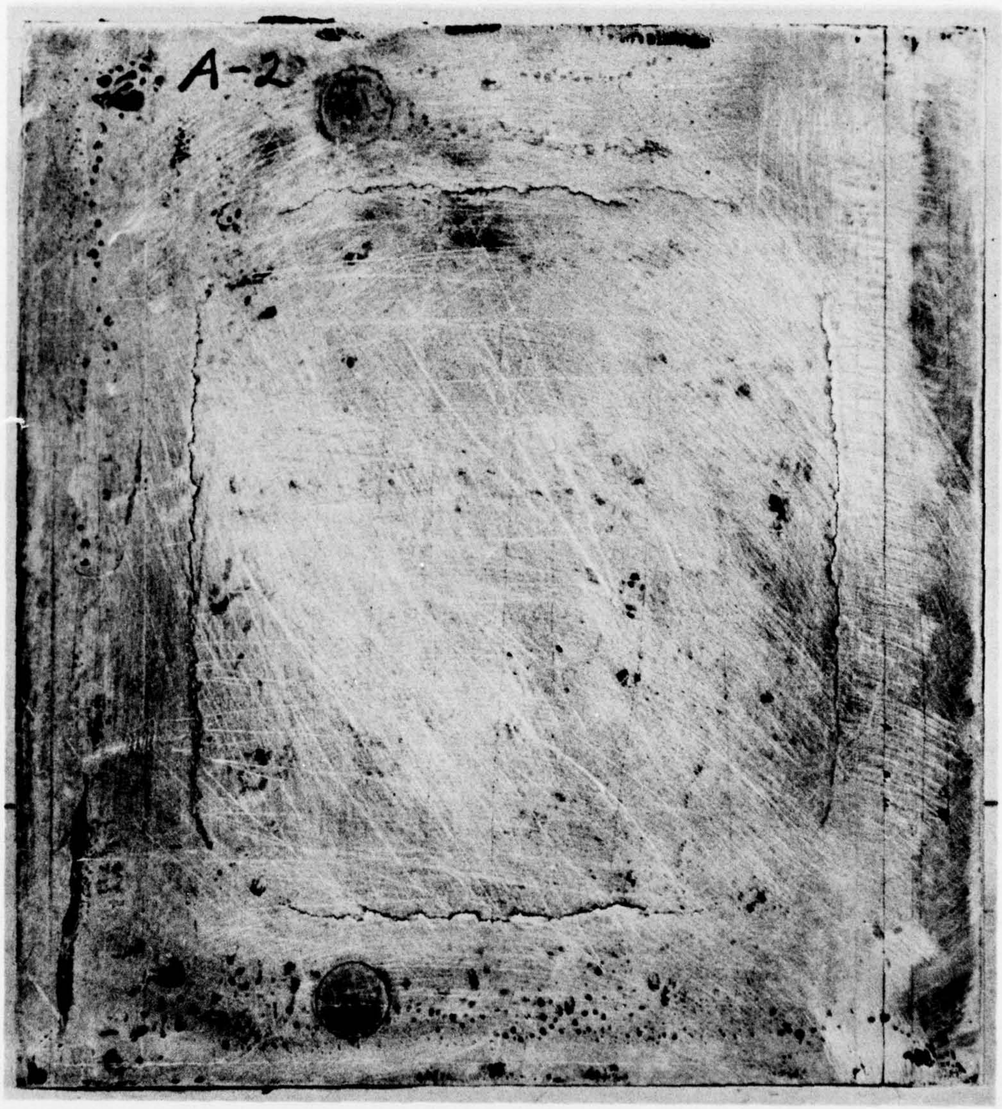

Fig. 1(b) - Transducer TR11-C #1

UNCLASSIFIED

[redacted]

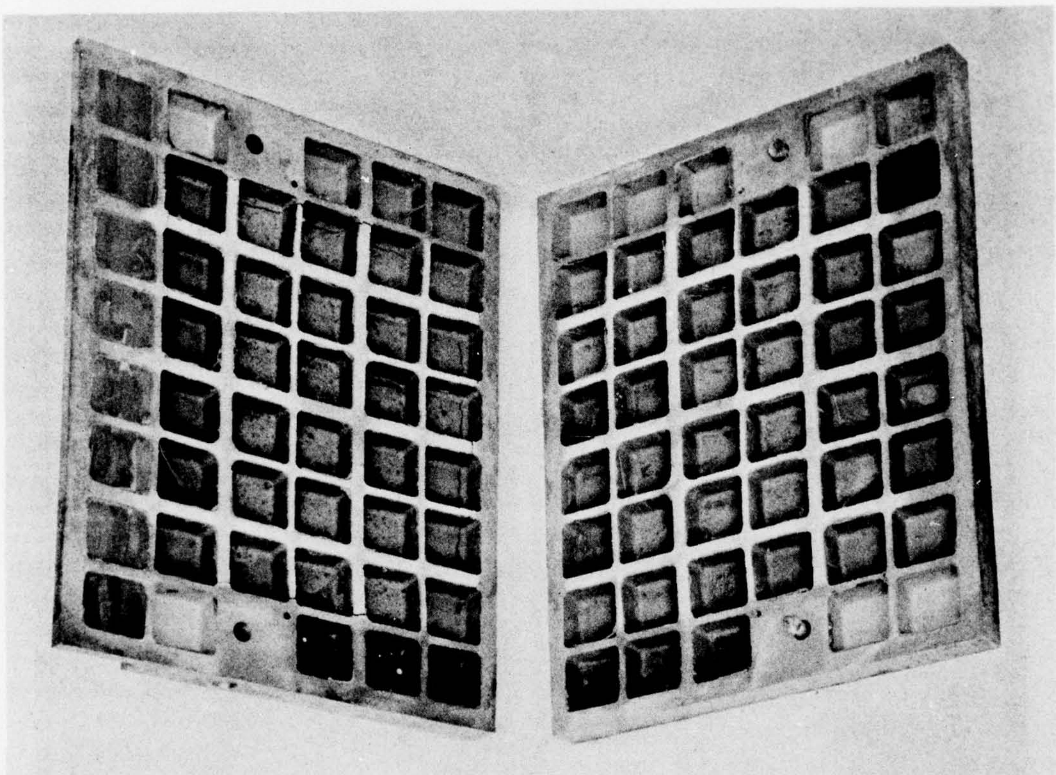

Fig. 2 - Split Plate of Transducer TR11-C #3

UNCLASSIFIED

[redacted]

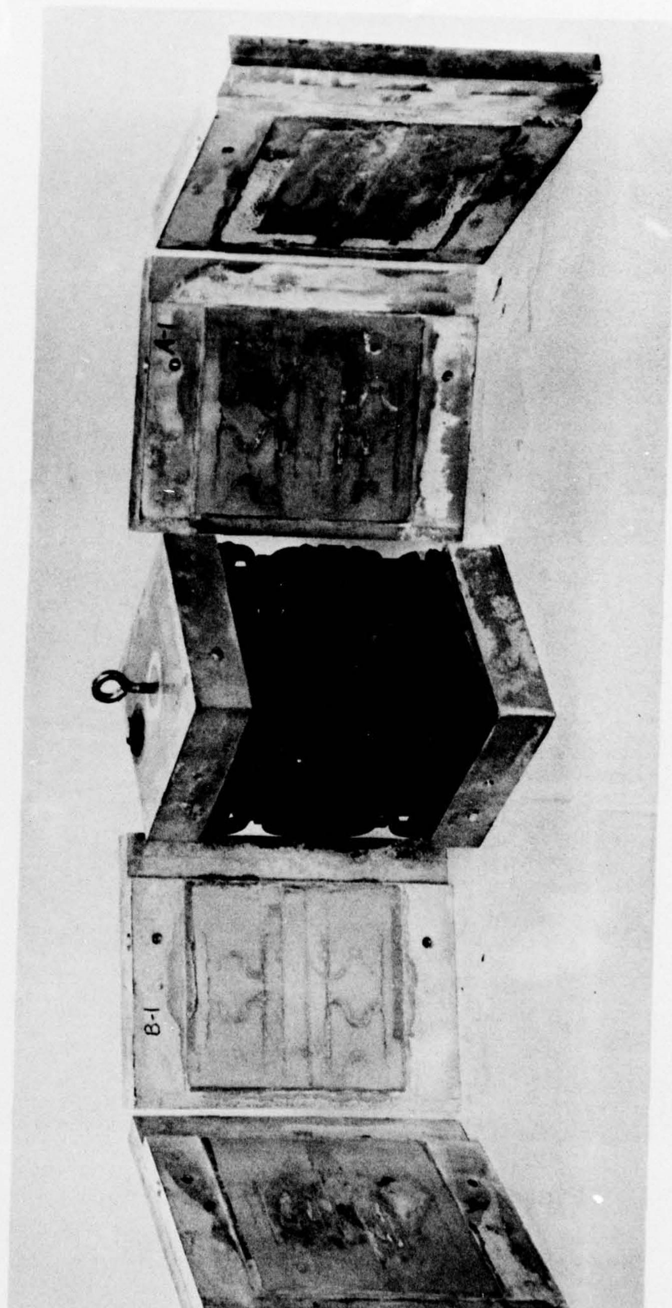

Fig. 3 - Transducer TR11-C #3

UNCLASSIFIED

[redacted]

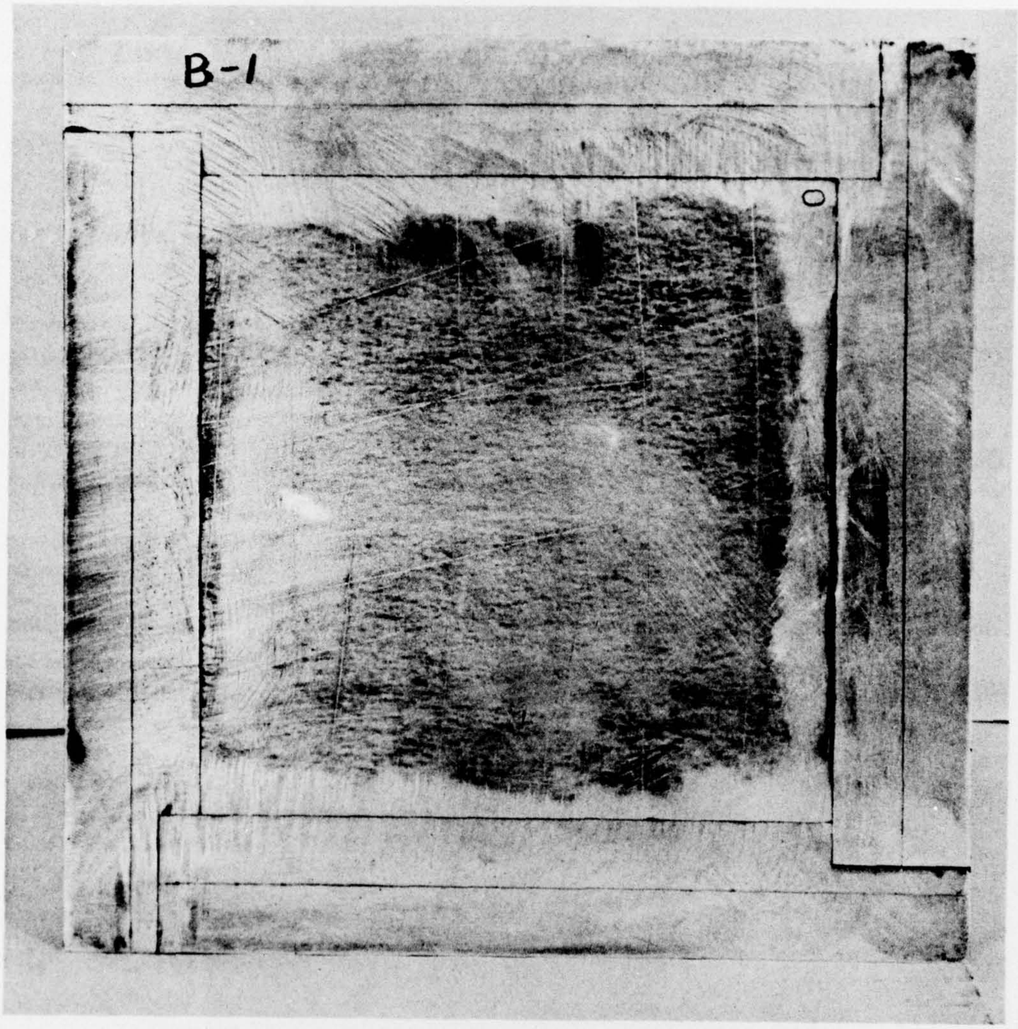

Fig. 4 - Transducer TR11-C #3